Environ Geol (2005) 48: 265–275
DOI 10.1007/s00254-005-1318-y

ORIGINAL ARTICLE

M. L. Lin
F. S. Jeng
L. S. Tsai
T. H. Huang

Wetting weakening of tertiary sandstones—microscopic mechanism

Received: 28 December 2004
Accepted: 19 April 2005
Published online: 18 June 2005

M. L. Lin · F. S. Jeng (✉)
L. S. Tsai · T. H. Huang
Department of Civil Engineering,
National Taiwan University, Taiwan
E-mail: fsjeng@ntu.edu.tw
Tel.: +886-2-23630530
Fax: +886-2-23645734

Abstract The micromechanism accounting for wetting weakening of tertiary sandstones was studied. It was found that intragranular fracture prevails for all dry sandstones. However, when the sandstone is wet, intergranular fracture occurs for *Type B* sandstones. Therefore, one sandstone from *Type A* sandstones, MS1, and another from *Type B*, TK, were selected to further investigate the nature of the matrix. It was found that (1) for both sandstones, the major mineral components of the matrix are illite and kaolinite except that the MS1 sandstone has more chlorite; (2) leaching of matrix induced an increase of porosity and consequently results in leaching softening; and (3) among the mineral composition, chlorite is easiest to be dissolved and leached out and induces a more significant increase of porosity, which, in turn, results in a more significant leaching softening.

Keywords Fracture · Tertiary sandstone · Matrix · Wetting softening

Introduction

The term ''sandstone'' denotes a large class of sedimentary rocks with different mineral compositions, diagenetic process and ages or degree of diagenesis. This diverseness in rock-forming origins results in a great variety of rock properties, including the strength, deformability, permeability and resistance to weathering. The mechanical behavior of sandstones and its affecting factors have been explored (Azzoni et al. 1996; Bell and Culshaw 1993, 1998; Bell and Lindsay 1999; Bernabe et al. 1994; Chigira and Sone 1991; Clough et al. 1981; David et al. 1998; Handin and Hager 1957; Hawking and McConnell 1992). Corresponding classification systems or methods of estimating strength of sandstone were suggested by Barton et al. (1993), Dick et al. (1994), Erosy and Waller (1995), Fahy and Guccione (1979), Gunsallus and Kulhawy (1984), Howarth and Rowlands (1986), Shakoor and Bonelli (1991) and Ulusay et al. (1994).

How the sandstone was fractured, when subjected to external loading, has been studied (Zhang et al. 1990; Sangha et al. 1974; Menenaez et al. 1996). In summary, wetted sandstones may become softer and weaker than dry sandstones (Bell 1978; Turk and Dearman 1986; Dobereiner and De Freitas 1986; Dyke and Dobereiner 1991). The degree of wetting softening can be related to porosity (Turk and Dearman 1986) and matrix content or mineral composition (Hawkins and McConnell 1992). Wetting weakening is of concern when assessing the stability of a dry rock slope that can be wetted due to heavy rainfall, or when predicting the crown settlement of an excavating tunnel that can be wetted by seeping water inside the tunnel.

In Taiwan, tertiary sandstones have a digenetic age of no more than 70 million years and such relatively short rock forming period is insufficient to classify them as hard rocks. The typical strength of tertiary sandstones in Taiwan ranges from 10 MPa to 80 MPa (Jeng and Huang 1998). These tertiary sandstones were often characterized as medium to weak rocks and their mechanical behavior differs from that of many hard rocks.

Among the tertiary sandstones, discrepancies in their mechanical behavior must be recognized. Tertiary sandstones are classified into two types, *Type A* and *Type*

B, Fig. 1 (Jeng et al. 2004). The mechanical properties of *Type A* are close to those of hard rock except that *Type A* sandstone has more significant shear dilation. Nevertheless, *Type B* sandstone, compared to the *Type A* sandstone, is characterized with (Jeng et al. 2004):

1. Lower stiffness in bulk modulus and shear modulus.
2. Substantial amount of volumetric deformation can be induced by shearing, namely the so-called shear dilation phenomenon.
3. Wetting will significantly reduce both the strength and the stiffness of the *Type B* sandstone. A strength reduction ratio due to wetting, *R*, is accordingly defined as

$$R = \mathrm{UCS}_{\mathrm{dry}}/\mathrm{UCS}_{\mathrm{dry}} \quad (1)$$

where *UCS* is the uniaxial compressive strength. The *R* of *Type B* sandstone is defined to be greater than 0.5. *Type B* sandstone can be prone to tunnel squeezing.

This paper is directed toward finding the microscopic mechanism that accounts for the significant reduction of strength and stiffness. Cycles of leaching tests were also conducted to identify what components of matrix can be dissolved and to determine the consequences.

Set-up of experimental study

A total of 13 samples of sandstones were obtained from eight geological formations of northern Taiwan to be tested. These sandstones were deposited under marine, marine-terrestrial and littoral facies, and their geological ages range from Oligocene to Pliocene. The specimen size

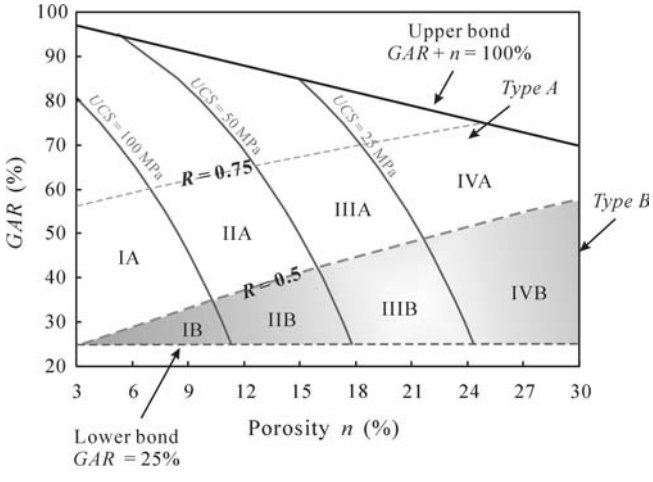

Fig. 1 Geotechnical classification of the studied sandstones in terms of *n* and GAR. The empirical UCS and *R* are shown by *solid* and *dashed contour lines*. The sandstones are classified into two groups: *Type A* ($R > 0.5$) and *Type B* ($R \leq 0.5$). The classification of strength (*Type I*, *II*, *III* and *IV*) is based on the definition of ISRM (1981)

was 5.5 cm in diameter and 12.5 cm in height. The specimen was oven dried (105°C) to remove its natural water content. For the uniaxial compression test, the axial load was provided by a servo-controlled high-stiffness machine, which had a maximum load and stiffness of 4448 kN and 13.1×10^9 N/m, respectively. The load is applied at a rate of 5 MPa/min. The longitudinal and transverse types of deformation were separately measured by a full Wheatstone bridge consisted of four strain gages, which were capable of measuring strains up to 2% with an accuracy of ± 0.85 (μm/m)/°C.

Since some of the tertiary sandstones exhibit wetting softening behavior, experiments were conducted on dry and wet specimens. The sandstones were soaked in water in a vacuum chamber for sufficient length of time (at least 24 h) so that the water content would stop increasing. Water was allowed to fill all the coalescent pores. Specimens, for the calcitic sandstones, should not be submerged in water too long to avoid dissolving and leaching of the minerals.

Petrographic features of the sandstones were accomplished by thin section analysis for better color contrast between grains and to identify grain boundaries. The size of area is chosen to include 80–150 grains in an image so that representative petrographic features can be observed. With these four types of images, the grain boundary, the matrix, the pore and the mineral composition of grains can be identified by computer and by visual recognition.

To study the relative mineral contents of matrix, both nonquantitative and semiquantitative X-ray diffraction tests (*XRD*) have also been conducted. Consequently, the relative mineral composition of matrix could be identified.

Scanning electron microscope (SEM) was used to observe the grains on the fracture surface (Oatley 1972). At least one piece of rock fragments was chipped from the fracture surface of dry or wet specimens, followed by coating of gold film, as observed under SEM. Broken grains on the fracture surface were thus identified and could reveal how the fracture surface was developed.

Furthermore, dry, thin section slides of rock specimens with a dimension of 2 cm×1 cm×1 cm were fractured by applying axial compression and observed under the microscope to notice the development of fracture surface. Comparing the fracture pattern observed by SEM to that of microscope, the validity of using SEM can be justified, provided that the results are consistent. Once the sandstone is fractured by uniaxial compression, the fractured specimen is cemented by epoxy glue and ground to a thin section to be observed under the microscope and grains fractured and the coalesced fracture surface can be observed.

As the properties and the components of matrix could inherently affect the macroscopic property and the wetting softening behavior of sandstones, cycles of

leaching test were also conducted on these sandstones to identify which components can be dissolved and how the mechanical properties are affected. The dissolved material was collected after 30 and 60 cycles of dry-and-wetting tests and analyzed by XRD to identify the relative contents of composition.

Basic Properties of tertiary sandstones

As shown in Table 1, the sandstones are mainly composed of quartz (greater than 75%) with the minor content of rock fragments and very little of feldspar (less than 5%); accordingly, these sandstones are classified as lithic graywacke or quartzwacke based on Pettijohn's definition (Pettijohn et al. 1987). The porosities range from 11% to 25%.

Figure 2 illustrates some of the petrographic images of the sandstones. In general, the grains have subrounded to subangular geometry. Some of the sandstones have a rather small grain ratio (*GAR* less than 50%), which implies a great portion of matrix and porosity.

The mechanical properties of sandstones, including uniaxial strength and *R* are listed in Table 2. A fairly wide spectrum of mechanical behavior was obtained, in which the dry and wet uniaxial compressive strengths varied from 7 to 86 MPa and 3 to 45 MPa , respectively.

Table 1 Compositions of sandstones studied (modified after Jeng et al. 2004)

Formation	*n* (%)	GAR (%)	Matrix (%)	PD	Mineralogy of grains		
					Quartz (%)	Feldspar (%)	Rock fragment (%)
WGS1	17.4	65.0	17.6	68.9	90.3	0.0	9.7
WGS2	16.7	25.3	58.0	44.9	85.8	0.0	7.2
MS1	11.5	50.4	38.2	–	88.0	0.2	10.3
MS2	14.1	67.5	18.5	74.2	90.7	0.2	9.0
MS3	13.1	51.0	35.9	65.4	85.0	2.3	12.2
TL1	13.1	36.4	50.5	56.2	86.5	1.7	9.9
TL2	12.8	50.0	37.2	67.0	87.3	0.7	9.7
ST	18.2	40.4	41.4	57.4	77.7	4.4	12.7
NK	14.8	28.6	56.6	55.2	90.0	2.3	5.6
TK	12.8	28.2	59.0	49.4	84.5	0.5	13.0
SFG1	24.6	52.6	22.8	73.6	95.6	0.8	3.0
SFG2	16.9	42.8	40.4	65.4	78.4	1.6	8.9
CL	20.7	39.4	40.0	61.2	83.7	1.0	5.5

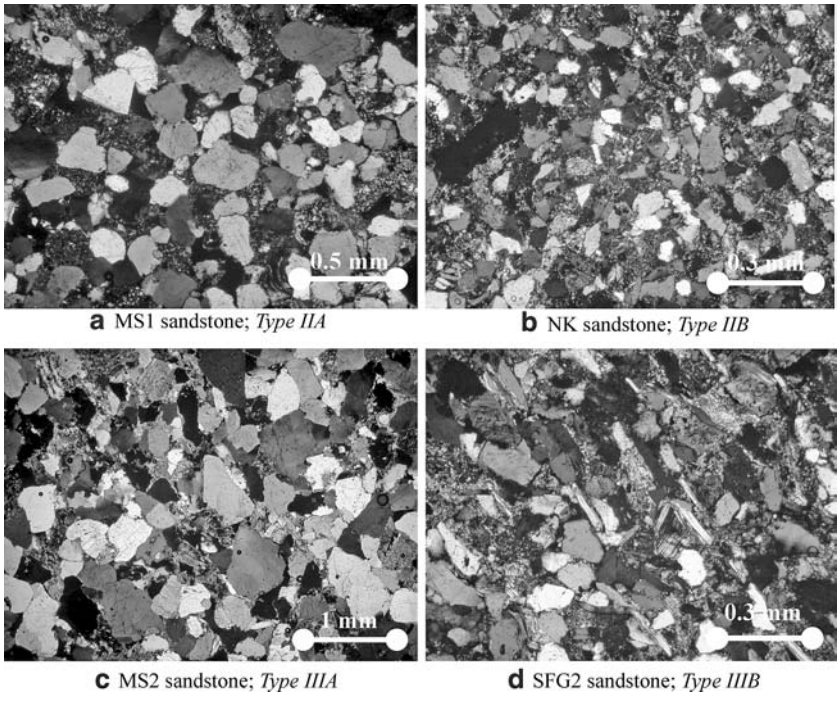

Fig. 2 Some of the typical petrographic images (crossed nickel) of the studied sandstones. A *white bar* shows the scale of each image. The symbols MS1, MS2, NK and SFG2 represent the stratum formation where the specimens came from. Figure 1 defines the rock types

Table 2 Mechanical properties of sandstones (modified after Jeng et al. 2004)

Formation	UCS_{dry} (MPa)	UCS_{wet} (MPa)	R	No. specimen	
				Dry	Sat
WGS1	34.1	25.4	0.74	8	9
WGS2	47.5	6.7	0.14	10	8
MS1	48.5	28.9	0.60	15	2
MS2	37.1	28.3	0.76	27	23
MS3	82.7	43.3	0.52	3	3
TL1	68.7	23.2	0.34	11	9
TL2	77.5	44.2	0.57	3	3
ST	38.4	7.8	0.20	5	3
NK	86.0	43.2	0.50	4	3
TK	69.0	29.4	0.43	10	2
SFG1	14.5	12.2	0.84	3	3
SFG2	46.4	19.9	0.43	3	3
CL	19.9	3.1	0.16	7	6

The strength reduction ratio R due to wetting softening is defined as $R = UCS_{wet}/CS_{dry}$

Remarkably, significant wetting softening could be observed, either in strength or in stiffness. The reduction ratio R ranged from 0.85 to as low as 0.14.

The relative mineral composition of the matrix for all sandstones is summarized in Table 3. The matrix is mainly composed of the illite, kaolinite and chlorite. A minor content of montmorillite can be found in some sandstones.

The UCS_{dry} can be expressed in terms of n and GAR as (Jeng et al. 2002):

$$UCS_{dry} = (133.7e^{-0.107n})(3.2 - 0.026GAR) \quad (2)$$

where the units for UCS, n and GAR are MPa, % and %. If the UCS expressed by Eq. 2 is defined as empirical UCS, it can be compared to the actual UCS, as shown in Fig. 3. In general, the actual UCS and the empirical UCS are consistent.

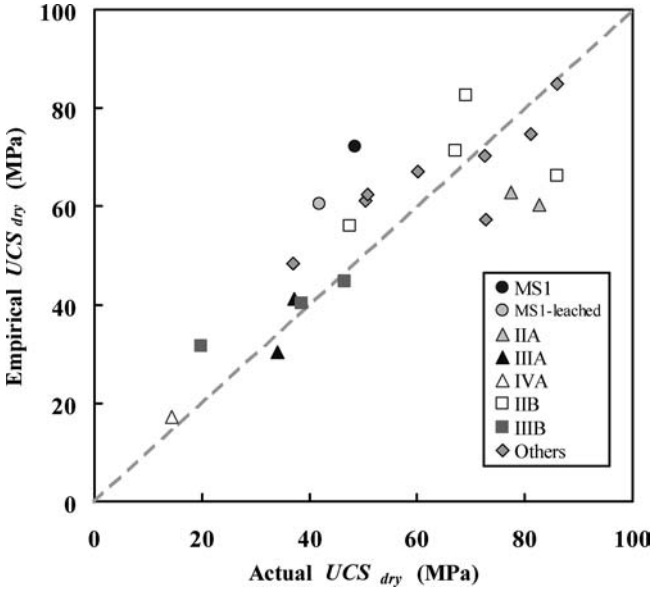

Fig. 3 Comparison of the empirical UCS (Eq. 1) and the actual UCS

Fracture behavior of tertiary sandstones

The fracture surfaces of the studied sandstone are shown in Fig. 4. It reveals that fracture grains can often be

Table 3 Mineral contents of the matrix for each type of sandstone (modified after Jeng et al. 2004)

Formation	Illite (%)	Kaolinite (%)	Chlorite (%)	Montmorillite (%)	Mixed layer (%)	Type[a]
WGS1	72	14	2	4	8	*IIIA*
WGS2	73	3	0	15	9	*IIB*
MS1	39	50	11	0	–	*IIA*
MS2	75	7	1	4	13	*IIIA*
MS3	69	11	19	0	–	*IIA*
TL1	32	14	6	6	42	*IIB*
TL2	16	30	54	0	–	*IIA*
ST	21	64	15	0	–	*IIIB*
NK	46	44	10	0	–	*IIB*
TK	60	40	1	0	–	*IIB*
SFG1	17	59	23	1	–	*IVA*
SFG2	20	56	24	0	–	*IIIB*
CL	35	8	3	27	27	*IIIB*

[a]Figure 1 defines the types of sandstone and the strength types (*I*, *II*, *III* and *IV*) are classified based on ISRM (1981)

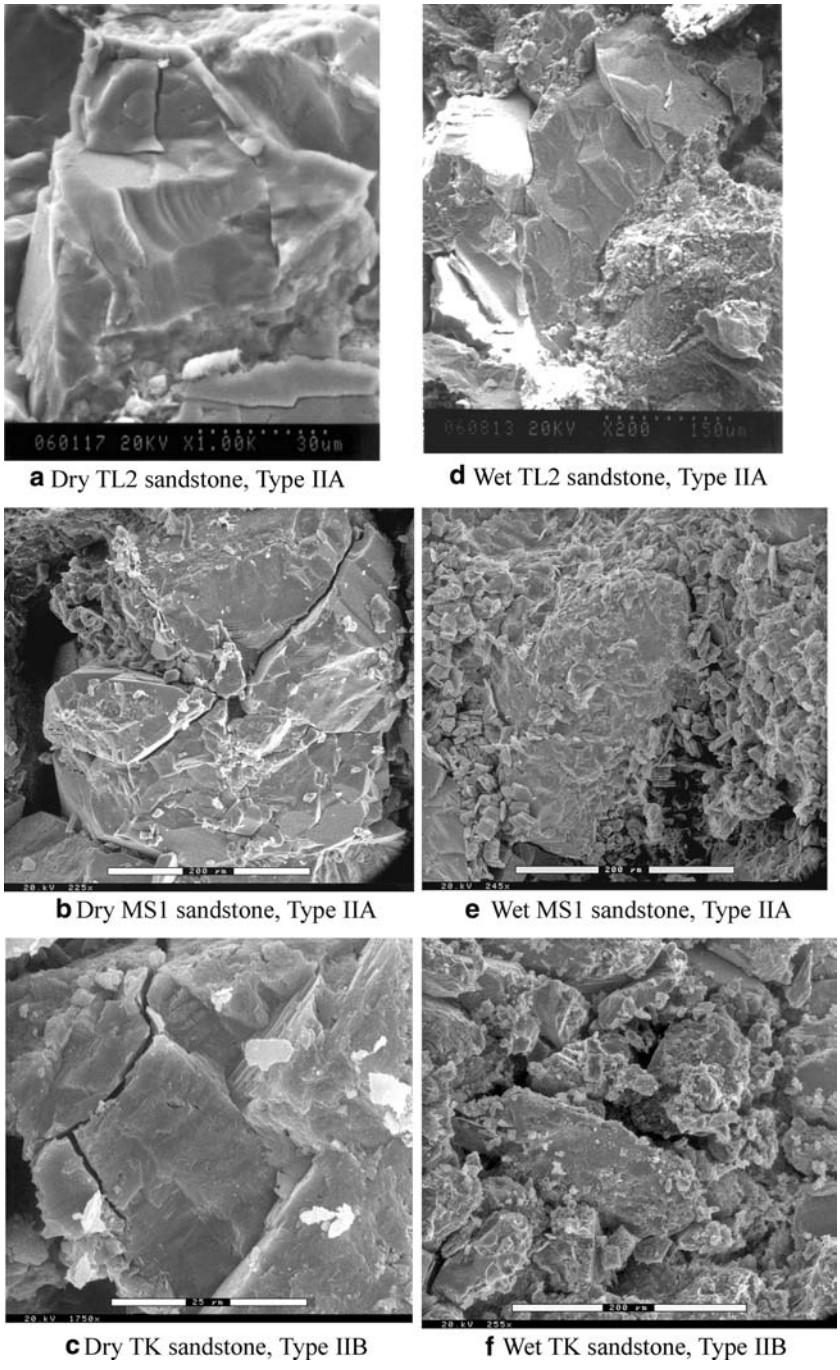

Fig. 4 Typical SEM images of fractures surfaces studied sandstones. The classification of sandstones is defined by Fig. 2b. The left and the right column of images are fracture surface obtained from dry and wet sandstones, respectively. The geotechnical properties of the sandstone shown in this figure are listed in Tables 1, 2, 3 and 4

found on the fracture surface of dry sandstones regardless of *Type A* or *Type B* sandstone (Figs. 4a, b, c). That is, the fracture surface is a result of coalescence of intragranular microcracks for all dry sandstones.

When the sandstone is wet, however, all the grains on the fracture surface remain intact for *Type B* sandstone. As the fracture surface is formed by coalescence of intergranular (or trans-matrix) cracks instead of intragranular ones (Fig. 4f). This phenomenon concurs with the finding by Dobereiner and De Freitas (1986).

For the intergranular type of fracture, the matrix is relatively softer than the grain and grains rotate during fracture process so that stress concentration will not be induced within the grains, fracture surface only tracks through the matrix without passing through the grains and eventually induces no grain breakages.

For *Type A* sandstone, however, intragranular fracture still prevails except for the MS1 sandstone, as listed in Table 4. Therefore, the fracture mechanism of *Type A* sandstone is not changed whether it is dry or wet.

The above-mentioned phenomena naturally render a scenario interpreting why *Type B* sandstone exhibits a greater wetting softening behavior than *Type A* does. When both types of sandstones are dry, the matrix seems to be strong enough to hold the grains in position; these grains are broken during the fracturing process. When sandstone is wetted, the matrix of *Type B* sandstone becomes much softer than the grains, which results in an trans-matrix fracture and to a much lower compressive strength with a strength reduction ratio $R \leq 0.5$. The wetting of *Type A* sandstones however, does not seem to induce sufficient matrix softening to transform the fracture type from intragranular to intergranular. Remarkably, some degree of strength reduction still occurs for *Type A* sandstone; however, the degree of wetting softening is less severe for *Type A* than *Type B*, which implies that the softening of matrix could still exist for *Type A* sandstone.

The observation obtained from tests of slice specimens confirms the aforementioned findings. As illustrated by Figs. 5a, b, intergranular fracture and intragranular fracture do actually happened for dry *Type B* and *Type A* sandstones, respectively.

Weakening due to leaching

The above-mentioned experimental results reveal that wetting softening of matrix would account for the *Type A* or *Type B* behavior. Therefore, one sandstone was selected from each type of sandstone, MS1 from *Type A* sandstone and TK from *Type B* sandstone, to study the wetting softening behavior and the effect of leaching.

When these two sandstones were submerged in water over various length of time, the degree of saturation increased with submergence time. Both the strength and the stiffness of the two sandstones decrease upon greater degrees of saturation, as shown by Figs. 6 and 7. For MS1 sandstone, the strength (UCS) reduces from 80 MPa to 30 MPa and a 63% decrease of strength, from a dry state to a completely wet state as shown in Fig. 6a. Similarly, a 40% decrease of strength occurs when the dry TK sandstone is wetted as illustrated by Fig. 6b. The reduction of stiffness is also significant; about a 60% loss of stiffness (Young's modulus) occurs for both sandstones, as depicted by Figs. 7a, b.

Although both MS1 and TK sandstones exhibit wetting softening behavior, the leaching effects of these two sandstones are somewhat different. The strength of TK sandstone does not seem to be affected by at least 60 cycles of dry–wet process as shown in Fig. 8. However, the MS1 sandstone loses 20% of strength after 60 dry–

Table 4 Fracture type of studied sandstones and corresponding properties

Formation	Grain (%)	Matrix (%)	Porosity (%)	UCS_{dry} (MPa)	UCS_{wet} (MPa)	Strength reduction ratio (R)	Rock group	Fracture type	
								Dry	Wet
SFG1	52.6	22.79	24.6	14.5	12.2	0.84	A	Intragranular	Intragranular
MS2	67.5	18.5	14.1	37.1	28.3	0.76	A	Intragranular	Intragranular
MS1	50.4	38.2	11.5	48.5	28.9	0.60	A	Intragranular	Intergranular
TL2	50.0	37.20	12.8	77.5	44.2	0.57	A	Intragranular	Intragranular
MS3	51.0	35.9	13.1	82.7	43.3	0.52	A	Intragranular	–
NK	28.6	56.62	14.8	86.0	43.2	0.50	B	Intergranular	Intergranular
TK	28.2	59.04	12.8	69.0	29.4	0.43	B	Intragranular	Intergranular
SFG2	42.8	40.36	16. 9	46.4	19.9	0.43	B	Intragranular	Intergranular
ST	40.4	41.45	18.2	38.4	7.8	0.20	B	Intragranular	Intergranular

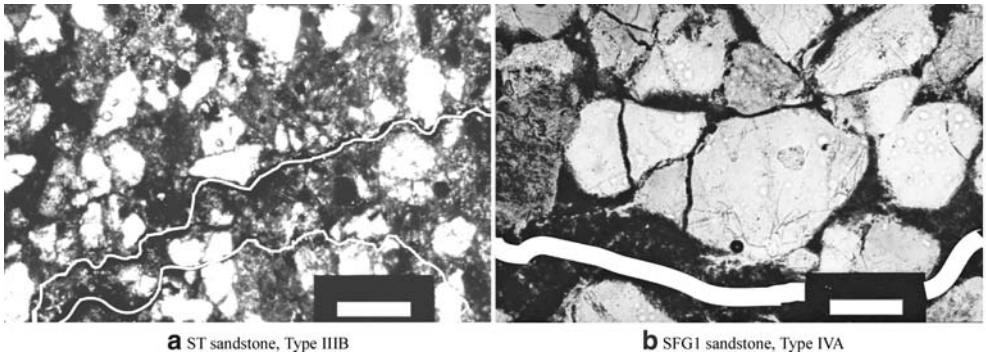

Fig. 5 Fracture surface obtained from tests on thin slice specimens. *Thick white lines* mark the major fracture surface. Intergranular fracture occurred for *Type B* sandstone (**a**), while intragranular fracture occurred in *Type A* sandstone (**b**). In **b**, microcracks within grains can be seen

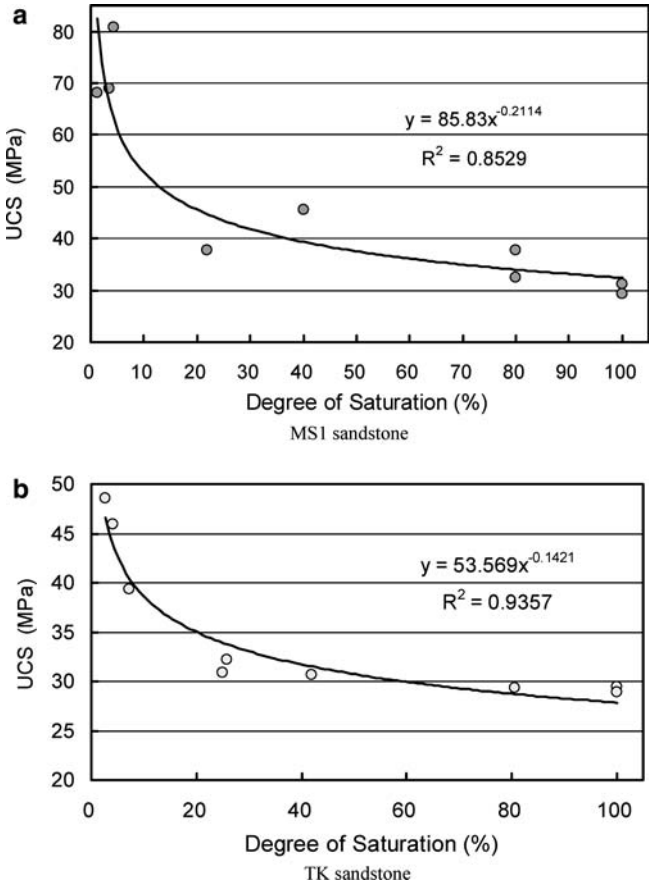

Fig. 6 Variation of UCS with degree of saturation for MS1 sandstone (**a**) and TK sandstone (**b**)

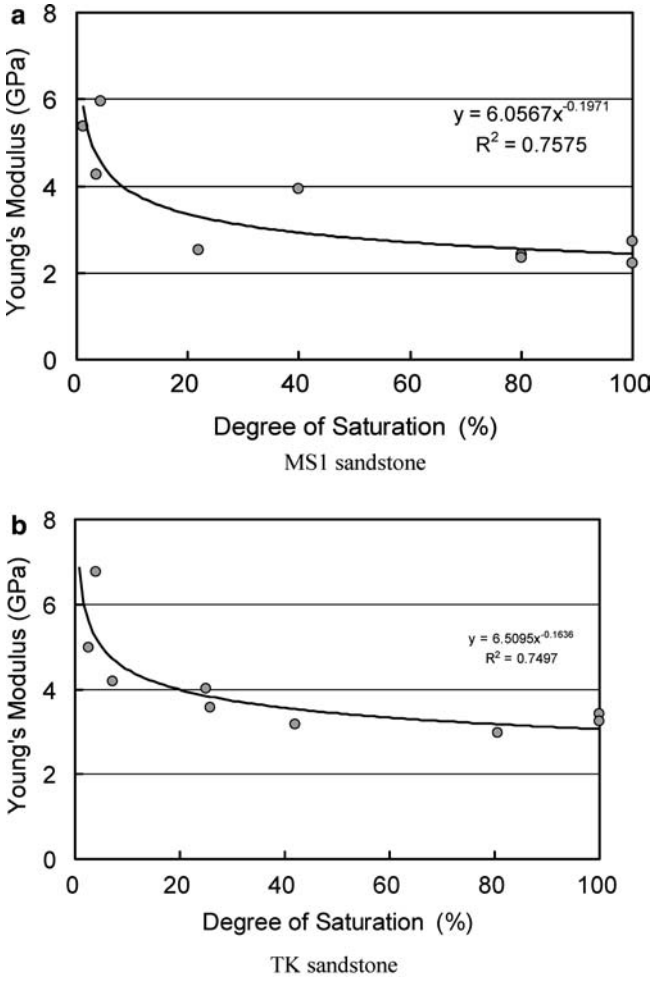

Fig. 7 Variation of Young's modulus with degree of saturation for MS1 sandstone (**a**) and TK sandstone (**b**)

wet cycles. The phenomenon implies that the matrix of MS1 sandstone, which leads to a wet intergranular fracturfe similar to *Type B* sandstone, of MS1 sandstones is easier to be ''leached out'' than the matrix of TK sandstone. A further examination of the porosity before and after leach tests confirmed this assertion. The porosity and density of TK sandstone remain unchanged after 60 cycles of dry–wet process. However, significant reduction of matrix content occurred for MS1 sandstone (Fig. 9a), which led to an obvious increase of porosity as shown in Fig. 9b. Apparently, the matrices of the two sandstones have different resistances to cycles of leaching. At this point, what accounts for such discrepancy should be further examined.

Before looking into the matrix, the microstructure of these two sandstones should be evaluated. As listed in Table 5a, these two sandstones have similar packing, types of contact and fracture feature; however, the grain size of TK sandstone is smaller. It is about 1/5 of the MS1 sandstone grain. The influence of wetting cycles on the two sandstones is summarized in Table 5, panel b, and about 0.13% and 0.09% (in weight) of matrix material has been leached out from MS1 and TK sandstones, respectively. The leached-out material was dried and tested using XRD to study its mineral content, as shown in Fig. 10. Results of XRD tests revealed the mineral content of the dissolved matrix, as shown in Fig. 11. Figure 11 indicates that

1. The major mineral components of the matrix are illite and kaolinite for both sandstones. However, the MS1 sandstone appears to have much more chlorite (about 10% before leaching) than the TK sandstone does.
2. After leaching test, the chlorite appears easier to be washed out than the other two minerals, illite and kaolinite. The relative content increases from 10% and 0.7% to 25.2% and 7% for MS1 and TK sandstones, respectively.

The mineral content of the matrix highlights that chlorite could be the key factor that makes the matrix different and thus account for the discrepancy in leaching effects. Meanwhile, chlorite is more easily affected by

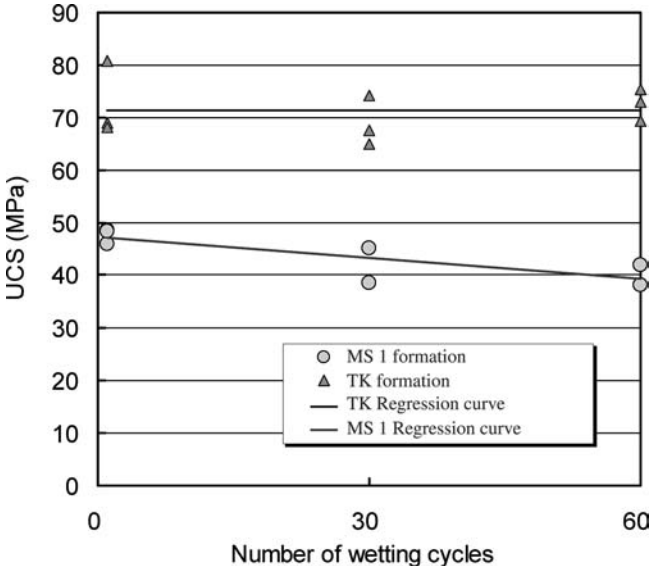

Fig. 8 Influence of wetting cycles to UCS obtained from MS1 and TK sandstones

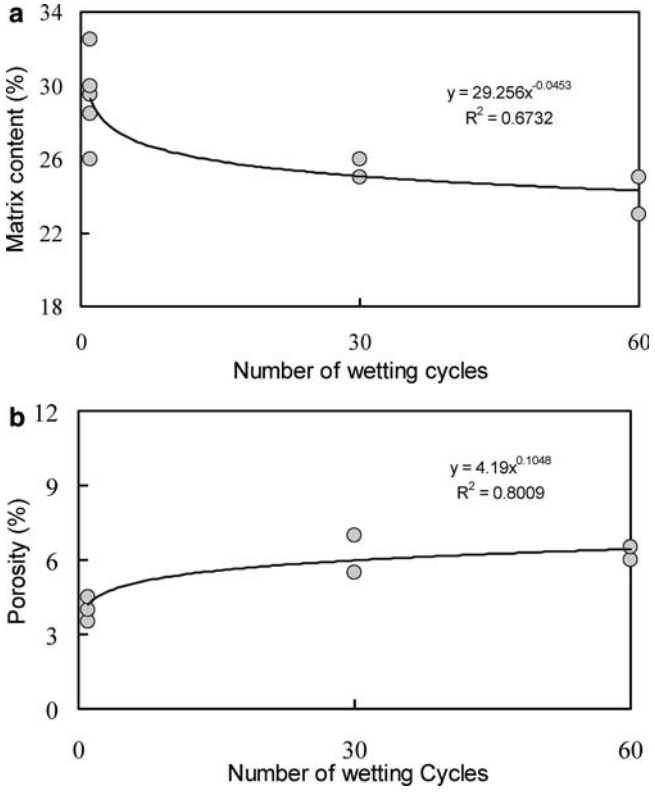

Fig. 9 Influence of wetting cycles to matrix content and the porosity of MS1 sandstone. More number of cycles reduces the matrix content (**a**), and increases the porosity (**b**)

Table 5 Comparison of MS1 and TK sandstones

		MS1 sandstone	TK sandstone
Comparison of microstructure			
Typical grain size		0.2 mm	0.04 mm
Microstructure	Packing	Contact 92.0%No contact 8.0%	Contact 79.9 %No contact 20.1%
	Types of grain contact	Tangential contact 61.0%Linear and suture contact 31.0%	Tangential contact 66.7% Linear and suture contact 13.2%
Fracture feature	Dry rock	Intragranular fracture prevails	
	Wetted rock	Intergranular fracture prevails	
Influences of wetting cycles			
(1) Compressive strength		Decrease 85%	Not effected
(2) Dry density		Before: 2.24 g/cm^{3}Aafter: 2.19 g/cm^3	Not affected
(3) Other changes		Significant decrease of matrix content and increase of porosity	Not affected
(4) Grain contact	Type of packing	Not affected	Not affected
	Type of contact	Not affected	Not affected
(5) Leached-out material	Leached-out weight	5.04 g 0.13%	2.71 g 0.09%
	Clay minerals	More chlorite than illite and kaolinite was leached out	XRD peak values are not significant enough for identified

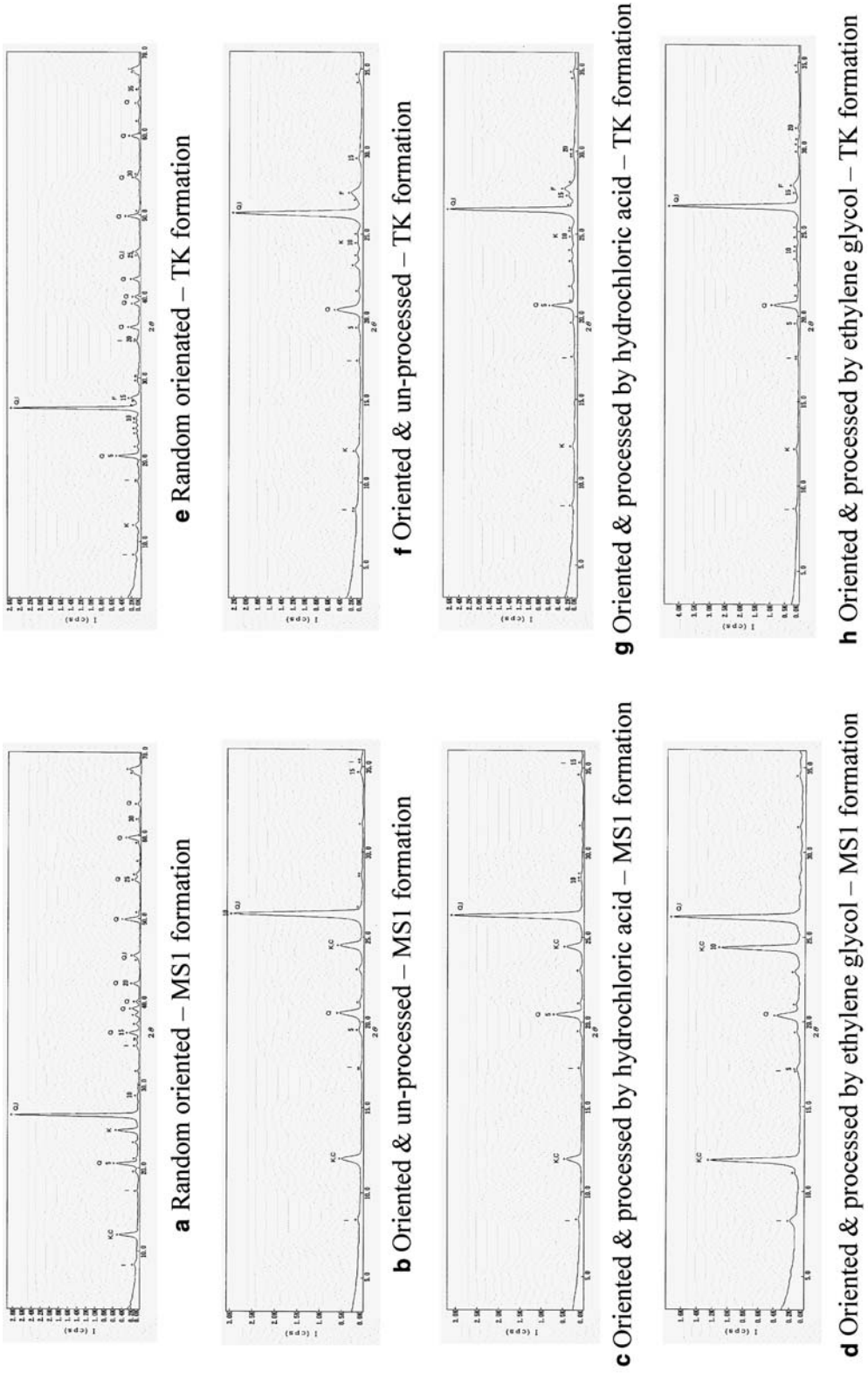

Fig. 10 Typical results of XRD for leach-out materials obtained from MS1 and TK formations

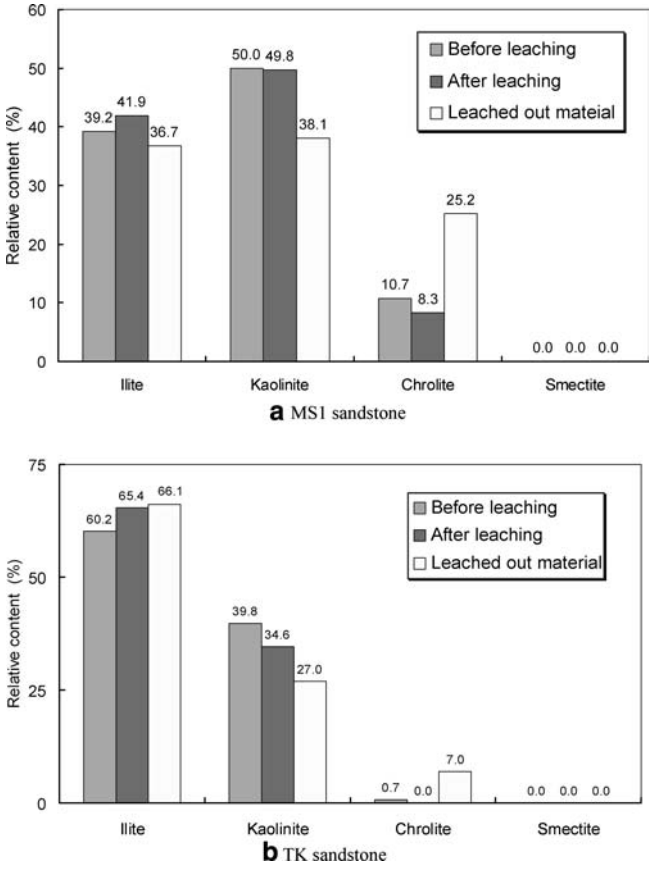

Fig. 11 Comparison of mineral contents for matrix before leaching, after leaching and the leached-out material. The number on top of each bar represents the relative contents (in weight) during the three phases of experiments. The sum of the relative contents for each color of bars is 100%

water than illite and kaolinite. It could also be the factor that induces intergranular fracture instead of trans-grain fracture of wet *Type A* sandstone.

Conclusion

The fracture patterns of *Type A* and *Type B* sandstones were investigated based on observations of fracture surface under SEM and on tests on thin slices of the sandstones observed under the microscope. It was found that intragranular fracture prevails for all dry sandstones. However, when the sandstone is wet, intergranular fracture occurs primarily in *Type B* sandstone. Considering the macroscopic mechanical behavior of sandstones, the strength and stiffness of dry sandstone is reduced when it is wet and *Type B* sandstone tends to have more significant wetting softening than *Type A* sandstone does. The intergranular fracture possibly enables an easier coalescence of microcracks so that *Type B* sandstone is more sensitive to wetting.

Study of the mineral composition of matrix found that chlorite is dissolved and leached out easier and that the porosity of sandstone increases and leads to a strength reduction. Special attention should thus be put on chlorite content of the matrix when allocating possible problematic sandstones. In addition to the factors found by previous research, including *GAR* and *n*, the nature of matrix appears to have influence on determining the behavior of sandstone to be *Type A* or *Type B*.

Acknowledgements The research is supported by the National Science Council of Taiwan, grant no. NSC-89-2211-E-002-152.

References

Azzoni A, Bailo F, Rondena E, Zaninetti A (1996) Assessment of texture coefficient for different rock types and correlation with uniaxial compressive strength and rock weathering. Rock Mech Rock Eng 29:39–46

Barton ME, Mockett LD, Palmer SN (1993) An engineering geological classification of the soil/rock borderline materials between sands and sandstones. In: Cripps JC, Coulthard JM, Culshaw MG, Forster A, Hencher SR, Moon CF (eds) The engineering geology of weak rock, vol 8. The Engineering Group of the Geological Society Special Publication, pp 125–138

Bell FG (1978) The physical and mechanical properties of the Fell Sandstones, Northumberland, England. Eng Geol 12:1–29

Bell FG, Culshaw MG (1993) A survey of the geotechnical properties of some relatively weak Triassic sandstones. The Engineering Geology of Weak Rock, pp 139–148

Bell FG, Culshaw MG (1998) Petrographic and engineering properties of sandstones from the Sneinton Formation, Nottinghamshire, England. Quart J Eng Geol 31:5–19

Bell FG, Lindsay P (1999) The petrographic and geomechanical properties of sandstones from the Newspaper Member of the Natal Group near Durban, South Africa. Eng Geol 53:57–81

Bernabe Y, Fryer DT, Shively RM (1994) Experimental observations of the elastic and inelastic behaviour of porous sandstones. Geophys J Int 117:403–418

Chigira M, Sone K (1991) Chemical weathering mechanisms and their effects on engineering properties of soft sandstone and conglomerate cemented by zeolite in a mountainous area. Eng Geol 30:195–219

Clough GW, Sitar N, Bachus RC, Rad NS (1981) Cemented sands under static loading. J Geotech Eng 107(GT6):799–817

David C, Menendez B, Bernabe Y (1998) The mechanical behaviour of synthetic sandstones with varying brittle cement content. Int J Rock Mech Min Sci Geomech Abstr 35(6):759–770

Dick JC, Shakoor A, Wells N (1994) A geological approach toward developing a mudrock-durability classification system. Can Geotech J 31:17–27

Dobereiner L, De Freitas MH (1986) Geotechnical properties of weak sandstone. Geotechnique 36(1):79–94

Dyke CG, Dobereiner L (1991) Evaluating the strength and deformability of sandstones. Quart J Eng Geol 24:123–134

Erosy A, Waller MD (1995) Textural characterisation of rock. Eng Geol 39:123–136

Fahy MP, Guccione MJ (1979) Estimating strength of sandstone using petrography thin-section date. Bull Assoc Eng Geol 16:467–485

Gunsallus KL, Kulhawy FH (1984) A comparative evaluation of rock strength measures. Int J Rock Mech Min Sci Geomech Abstr 21:233–248

Handin J, Hager RV (1957) Experimental deformation of sedimentary rock under a confining pressure. J Am Assoc Pet Geol 41:1–50

Hawkins AB, McConnell BJ (1992) Sensitivity of sandstone strength and deformability to changes in moisture content. Quart J Eng Geol 25:115–130

Howarth DF, Rowlands JC (1986) Development of and index to quantify rock texture for qualitative assessment of intact rock properties. Geotech Testing J 9(4):169–179

ISRM (1981) Rock characterization testing and monitoring. In: Brown ET (ed) ISRM Suggested Methods. Pergamon, New York, p 211

Jeng FS, Huang TH (1998) Shear dilatational behavior of weak sandstone. In: Proc of Regional Symposium on Sedimentary Rock Engineering, Taipei, pp 262–267

Jeng FS, Weng MC, Huang TH, Lin ML (2002) Deformational characteristics of weak sandstone and impact to tunnel deformation. Tunnel Underground Space 17:263–274

Jeng FS, Weng MC, Lin ML, Huang TH (2004) Influence of petrographic parameters on geotechnical properties of tertiary sandstones from Taiwan. Eng Geol 73:71–91

Menenaez B, Zhu W, Wong T-F (1996) Micromechanics of brittle faulting and cataclastic flow in Berea Sandstone. J Struct Geol 18:1–16

Oatley CW (1972) The scanning electron Microscope. Cambridge University Press

Pettijohn FJ, Potter PE, Siever R (1987) Sand and sandstone. Springer-Verlag, Berlin

Sangha CM, Talbot CJ, Dhir RK (1974) Microfracturing of a sandstone in uniaxial compression. Int J Rock Mech Min Sci Geomech Abstr 11:107–113

Shakoor A, Bonelli RE (1991) Relationship between petrographic characteristics, engineering index properties and mechanics properties of selected sandstone. Bull Assoc Eng Geol 28:55–71

Turk N, Dearman WR (1986) Influence of water on engineering properties of weathered rocks. Groundwater Eng Geol, London, pp 131–138

Ulusay R, Tureli K, Ider MH (1994) Prediction of engineering properties of selected Litharenite sandstone from its petrographic characteristics using correlation and multivariate statistical techniques. Eng Geol 37:135–157

Zhang J, Wong T-F, Davis DM (1990) Micromechanics of pressure-induced grain crushing in porous rocks. J Geophys Res 95(B1):341–352